nature structural & molecular biology

Chemomechanical coupling in F_1-ATPase revealed by simultaneous observation of nucleotide kinetics and rotation

Takayuki Nishizaka[1,2,7], Kazuhiro Oiwa[1], Hiroyuki Noji[3], Shigeki Kimura[1], Eiro Muneyuki[4], Masasuke Yoshida[4,5] & Kazuhiko Kinosita Jr[6]

F_1-ATPase is a rotary molecular motor in which unidirectional rotation of the central γ subunit is powered by ATP hydrolysis in three catalytic sites arranged 120° apart around γ. To study how hydrolysis reactions produce mechanical rotation, we observed rotation under an optical microscope to see which of the three sites bound and released a fluorescent ATP analog. Assuming that the analog mimics authentic ATP, the following scheme emerges: (i) in the ATP-waiting state, one site, dictated by the orientation of γ, is empty, whereas the other two bind a nucleotide; (ii) ATP binding to the empty site drives an ~80° rotation of γ; (iii) this triggers a reaction(s), hydrolysis and/or phosphate release, but not ADP release in the site that bound ATP one step earlier; (iv) completion of this reaction induces further ~40° rotation.

The enzyme F_oF_1-ATP synthase catalyzes the synthesis of ATP from ADP and phosphate using proton-motive force across a membrane. The F_1 sector has catalytic sites responsible for the synthesis reaction; when isolated, it solely hydrolyzes ATP, and is thus called F_1-ATPase. F_1 contains five different subunits with the stoichiometry $\alpha_3\beta_3\gamma\delta\varepsilon$: the central stalk γ is surrounded by a hexagonal cylinder in which three α and three β subunits are alternately arranged[1]. The catalytic sites are located at the interfaces between α and β subunits, mainly on a β subunit, and are thus arranged 120° apart around the γ subunit. It has been proposed that the synthesis reactions in the three catalytic sites occur not independently but sequentially, one site after another[2,3]. In this proposal's 'binding-change mechanism,' the three catalytic sites have different affinities for nucleotides at any moment, and each undergoes conformational transitions that lead to the sequence of substrate binding → ATP synthesis → ATP release. This mechanism was proposed to involve rotation of a shaft domain: proton-motive force is converted, in F_o, to mechanical rotation of the shaft, which drives conformational changes of the catalytic domains in F_1 to synthesize ATP. Conversely, hydrolysis of ATP induces reverse conformational changes, and thus reverse rotation of the shaft domain (reviewed in ref. 4). Rotation has ultimately been confirmed by direct observation as rotation of the γ subunit in an isolated $\alpha_3\beta_3\gamma$ subcomplex[5].

Observation of F_1 rotation under an optical microscope has clarified that rotation of the γ subunit is unidirectional and can be driven by hydrolysis of ATP, GTP or ITP[5,6], as well as that rotation is resolved into discrete 120° steps, each of which consumes one ATP molecule[7,8]. On the basis of these and previous biochemical studies, possible mechanisms of F_1 rotation have been discussed[9–11]. However, the precise correspondence between chemical reactions and mechanical rotation remains to be established, that is: which chemical event on which catalytic site drives a particular phase of rotation? This is not a trivial task, because both rotation and chemical reactions are stochastic, and because the three catalytic sites are basically identical. A recent high-speed imaging study has shown that a 120° step consists of ~90° and ~30° substeps, and that ATP binding drives the 90° substep[12]. However, the reaction that drives the 30° substep and the reactions that precede and govern its timing have not yet been identified. Here we have attempted to disentangle the complex relationships between chemical and mechanical events by imaging individual F_1 molecules under an optical microscope.

RESULTS

Distinguishing three catalytic sites by polarization

We visualized rotation by attaching a bead duplex to the γ shaft, and simultaneously detected binding of a fluorescent ATP analog to a particular site through angle-resolved fluorescence imaging (**Fig. 1**, and see **Supplementary Fig. 1** online for microscope diagram). We used the fluorescent ATP analog 2′-*O*-Cy3-EDA-ATP[13], which we refer to hereafter as Cy3-ATP.

[1]Kansai Advanced Research Center, Protein Biophysics Group, Iwaoka 588-2, Nishi-ku, Kobe 651-2492, Japan. [2]Precursory Research for Embryonic Science and Technology (PRESTO), Japan Science and Technology Agency, Honcho 4-1-8, Kawaguchi, Saitama 332-0012, Japan. [3]Institute of Industrial Science, University of Tokyo, Tokyo 153-8505, Japan. [4]Chemical Resources Laboratory, Tokyo Institute of Technology, Yokohama 226-8503, Japan. [5]ATP system, Exploratory Research for Advanced Technology (ERATO), Japan Science and Technology Agency, Yokohama 226-0026, Japan. [6]Center for Integrative Bioscience, Okazaki National Research Institutes, Myodaiji, Okazaki 444-8585, Japan. [7]Present address: Department of Physics, Gakushuin University, Mejiro 1-5-1, Toshima-ku, Tokyo 171-8588, Japan. Correspondence should be addressed to T.N. (takayuki.nishizaka@gakushuin.ac.jp).

Published online 18 January 2004; doi:10.1038/nsmb721

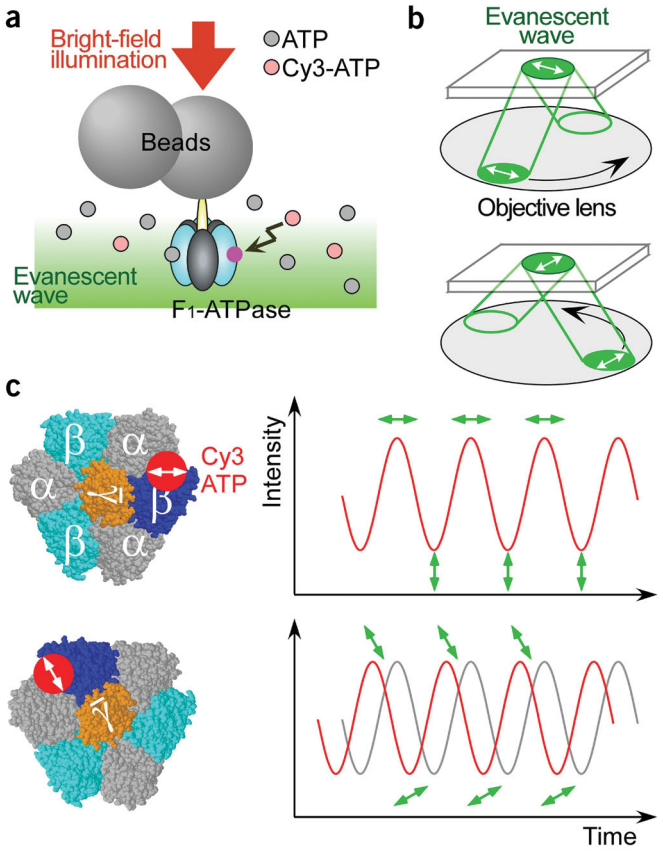

Figure 1 Experimental system. (**a**) Simultaneous-observation system (not to scale). Single turnovers of ATP hydrolysis on catalytic sites in F_1-ATPase are visualized with fluorescently labeled ATP (Cy3-ATP), which is excited by an evanescent wave under total internal reflection fluorescence microscopy. Rotation of a bead duplex attached to the γ shaft is simultaneously observed under bright-field illumination at a wavelength different from the emission of Cy3-ATP. (**b**) Schematic illustrations describing the optical system for angle-resolved imaging, with which we distinguish among the three catalytic sites on F_1 from Cy3 orientation. The incident laser is rotated along the periphery of the objective (black arrow), keeping its polarization parallel with the circular trajectory (white arrows). The direction of polarization of the evanescent wave is rotated within the image plane (white arrows at top). (**c**) Expected intensity time courses for a single Cy3-ATP molecule (right panels) bound to different catalytic sites 120° apart on F_1 (left). The fluorescence intensity (red curves) reaches maxima and minima when the excitation polarization becomes parallel and orthogonal, respectively (green arrows), to the absorption transition moment of the Cy3.

In this study, evanescent-wave excitation was realized by passing a laser beam through the edge of an objective in a method developed for visualization of single fluorophores[14]. Cy3-ATP appears as a stable fluorescent spot when it binds to a surface-immobilized F_1 molecule, whereas unbound Cy3-ATP is virtually invisible because of its rapid Brownian motion[15,16]. We rotated the polarization of the near-field excitation in the image plane at a constant speed by rotating the polarization of the incident laser beam and, at the same time, the beam itself along the periphery of the objective (**Fig. 1b**, and see **Supplementary Fig. 2** online for optical system; note that rotation of laser polarization alone, as done in far-field excitation[8,17,18], is insufficient because the evanescent wave has a small (<10%) polarization component along the direction of the incident laser beam between a numerical aperture of 1.33 and 1.45 (ref. 19). Under the rotating polarized excitation, fluorescence intensity from a single fluorophore is expected to show sinusoidal oscillation (**Fig. 1c**). The intensity reaches a peak every 180°, when the excitation polarization becomes parallel with the absorption transition moment of the fluorophore. Thus, we can determine the fluorophore orientation with the ambiguity of multiples of 180°. The three catalytic sites should host the fluorophore at three different angles that are 120° apart in the image (*x*-*y*) plane; therefore, a particular site binding a fluorescent ATP analog can be distinguished with this method.

Newly bound ATP dictates the orientation of the γ subunit

We used an $\alpha_3\beta_3\gamma$ subcomplex of F_1 with mutations that rendered the subcomplex much less prone to MgADP inhibition than the wild type (a 'GT' mutant; E.M., unpublished data; for details, see Methods). During ATP hydrolysis and rotation, F_1 becomes inactive by stochastic and tight binding of MgADP[20–22]; thus rotation lapses into long pauses. Because we wanted to observe repeated binding of Cy3-ATP to the same F_1 molecule, we used the GT mutant. The rotation rate of this mutant by authentic ATP was somewhat slower than that of the active (uninhibited) wild type, and rotation by Cy3-ATP was even slower (see below). Because other rotation characteristics seemed normal, we assume that the chemomechanical coupling in this mutant is basically the same as that of the wild type, and that Cy3-ATP induces the same series of events as authentic ATP, albeit slowly. In this study we sought to relate chemical events on the three catalytic sites with mechanical events, and thus here we disregard (until Discussion) the differences in absolute values of rate constants, assuming these differences are not the result of a grossly different reaction scheme. Another advantage of using the GT mutant was that we could observe substeps in its rotation under pure Cy3-ATP with a conventional video camera (**Fig. 4a**). The average rate of rotation of wild-type F_1 with Cy3-ATP was also slow, but we did not observe the video-rate substeps with the wild type. Below, we refer to the mutant subcomplex simply as F_1.

To allow, at most, one Cy3-ATP molecule at a time to bind, excess unlabeled ATP was added to Cy3-ATP. Before binding of Cy3-ATP, the bead duplex on the γ subunit rotated with clear counterclockwise 120° steps by unlabeled ATP (**Fig. 2a**). When a Cy3-ATP molecule bound to the F_1 molecule, a fluorescent spot appeared at the center of bead rotation, and began to blink regularly, indicating fluorophore angle.

We first observed that the binding of Cy3-ATP is synchronous with a 120° step (**Fig. 2b**; this example was chosen to show the intensity oscillations clearly, and therefore the total duration of Cy3-ATP binding is longer than most others). Second, while Cy3-ATP is still bound, the bead duplex makes another 120° step, indicating that a nucleotide is bound to F_1 for at least two-thirds of a revolution. Third, release of Cy3-nucleotide, presumably in the form of Cy3-ADP, is also synchronous with the third 120° step.

The fluorophore angle θ remained constant during each binding event, even though the γ subunit rotated by 120° in the middle (**Fig. 2a,b**; θ was 107 ± 2° in this binding-release event). Thus, this 120° step was not caused by the binding of another Cy3-ATP to a different site. As shown below, the expected rate of binding at 50 nM Cy3-ATP is once in 5 min, and thus successive binding of two Cy3-ATP molecules is extremely improbable.

In another binding event on the same F_1 molecule, the orientation of bound Cy3 and the bead orientation immediately after Cy3-ATP binding keep a fixed relationship, maintaining the same constant offset angle (compare right top panels in **Fig. 2b–d**; ~120° counterclockwise in this example). We summarize all results of simultaneous observation in which Cy3-ATP bound at least once to each of the three catalytic sites (**Fig. 2e**). The two (bead and Cy3) angles are well correlated without exception, reinforcing the contention that, as soon as a catalytic site binds ATP, the γ subunit always turns the same 'face'

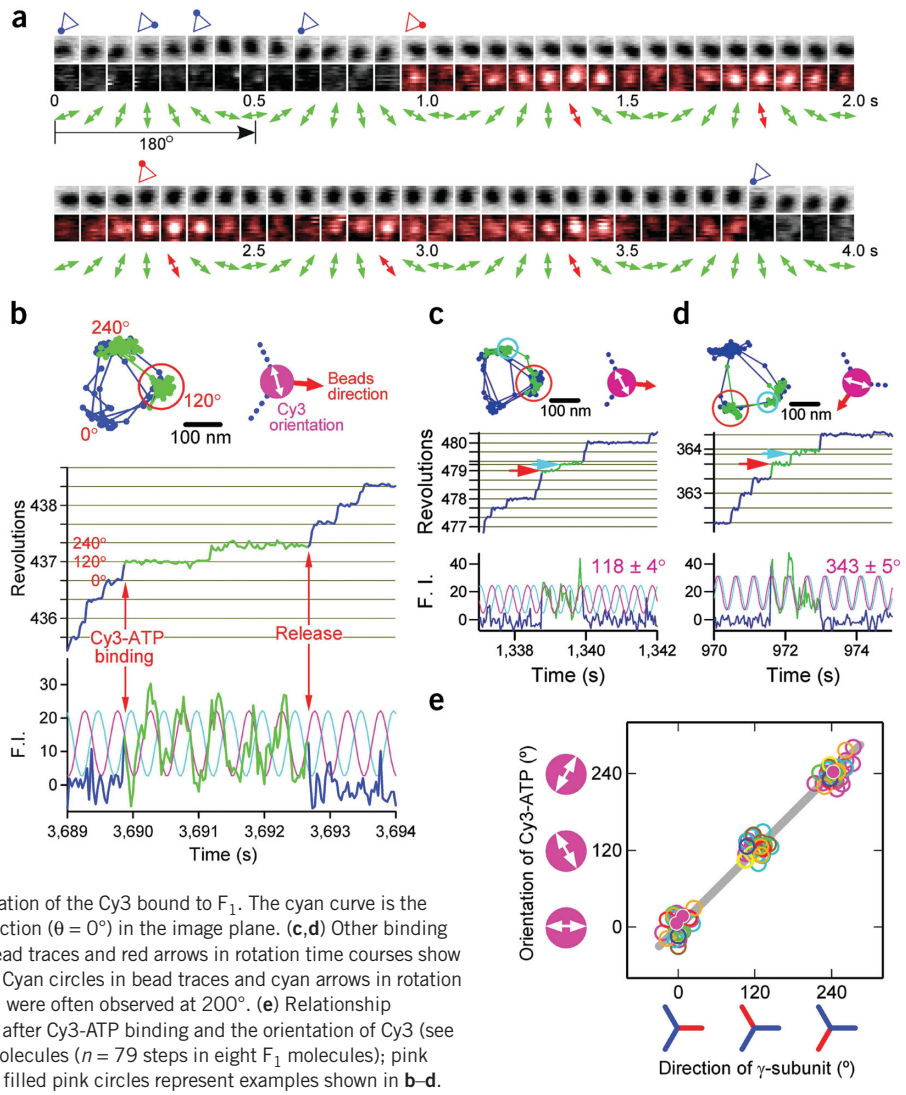

Figure 2 Simultaneous observation of F_1 rotation and Cy3-ATP binding. (**a**) Examples of simultaneous observation of bead stepping as bright-field images (upper rows) and Cy3-ATP binding as fluorescence images (lower rows) in a mixture of Cy3-ATP (50 nM) and excess unlabeled ATP (550 nM). Triangles above the image pairs indicate bead directions immediately after a counterclockwise step. The period during which one catalytic site in F_1 is occupied with Cy3-nucleotide (Cy3-ATP or product Cy3-ADP) is highlighted with red in the lower images. Green arrows below the image pairs show the orientation of the excitation polarization, and red arrows highlight the orientation when the fluorescence intensity becomes maximal and thus show the orientation of the bound Cy3. The bead orientation immediately after Cy3-ATP binding (the first red triangle) is near 3 o'clock, and the orientation of bound Cy3 (red arrows) is near 11 o'clock (equivalent to 5 o'clock) and ~120° counterclockwise (or 60° clockwise) from the bead orientation. Frame width, 0.7 μm for upper rows and 1.4 μm for lower rows. (**b**) Analyses of **a**. Left top, trace of bead motion. The centroid of the image of the bead duplex was calculated in each video frame (33 ms). Right top, diagram indicating the bead direction, and Cy3 orientation estimated from the bottom panel. Middle, time course of bead rotation. Time zero is the start of observation. The angle immediately before Cy3-ATP binding is designated 0°. Bottom, time course of the fluorescence intensity (F.I.) in the vicinity of the F_1 molecule. In **b**–**d**, the period during which Cy3-AT(D)P was judged bound to F_1 is highlighted in green. The green portion of the intensity time course is fitted with the pink curve representing $\cos^2(\omega t + \theta) \propto \cos(2\omega t + 2\theta)$, where ω is the angular rate of prism rotation and θ is the orientation of the Cy3 bound to F_1. The cyan curve is the reference representing a fluorophore lying in the *x* direction (θ = 0°) in the image plane. (**c**,**d**) Other binding events for the same molecule as in **a**. Red circles in bead traces and red arrows in rotation time courses show the angles immediately after Cy3-ATP binding (120°). Cyan circles in bead traces and cyan arrows in rotation time courses show pauses after an 80° substep, which were often observed at 200°. (**e**) Relationship between the direction of the bead duplex immediately after Cy3-ATP binding and the orientation of Cy3 (see Methods for details). Different colors show different molecules (n = 79 steps in eight F_1 molecules); pink circles are the same molecule as in **a**–**d**, and the three filled pink circles represent examples shown in **b**–**d**.

(the bar on γ in **Fig. 1c**) to the β subunit hosting that site. Conversely, the γ subunit dictates which of the three β subunits should bind the next ATP: it must be the β subunit that is 120° ahead from the face of γ. It has been shown that ATP binding drives ~90° rotation of the γ subunit, which is immediately (in ~2 ms) followed by ~30° rotation[12]. We show here that this ATP must bind to the particular β subunit dictated by the orientation of the central γ subunit.

Binding accompanies rotation

Because of the oscillation of fluorescence intensity and the inherent noise in single-fluorophore detection, we cannot be certain that we detected all binding events. Binding events that persisted for one oscillation cycle (0.5 s) or longer were clear, and we scored altogether 163 such events on 27 F_1 molecules. In 155 out of the 163 cases, a 120° step was observed in synchrony with the binding; when binding occurred in a dark phase of fluorescence oscillation, we could not be completely certain if the step was precisely synchronous, but all 155 steps were well within the first oscillation cycle (0.5 s) of the binding (see Methods for the exceptional eight cases). In 31 of the 155 binding events, binding of Cy3-ATP occurred near a peak of the intensity oscillation (within 20% of the peak intensity), allowing precise determination of the timing. In all 31 cases, a forward 120° step was observed within ±1 video frame (33 ms) of the binding (see examples in **Fig. 3a**). Combining this information with the angle determinations already made, we conclude that binding to the correct β subunit, dictated by the γ subunit, is required for a forward 120° step, and that binding immediately induces a rotational step.

Because the temporal resolution is limited to the video rate, one could argue that stepping might have preceded binding, and thus stepping could be the cause, rather than a result, of binding (as in a thermal-ratchet model[23–25]). Indeed, Brownian fluctuation could help bind ATP, because earlier work[12] has indicated that rotation in the correct (counterclockwise) direction increases the affinity for ATP, and thus rotation and binding are cooperative events. A full 120° step before ATP binding, however, must be extremely rare, judging from the size of angular fluctuations at low ATP concentrations. Also, we cannot claim that binding of Cy3-ATP or ATP invariably induces a 120° step: stepping initiated by binding of Cy3-ATP or ATP might immediately be reversed by premature release of the nucleotide, and such a brief binding associated with a small-amplitude mechanical pulse would not be detected in our video-rate analysis.

Cy3-nucleotide (presumably in the form of Cy3-ADP) was released, in 142 out of the 163 binding events, after the γ subunit had rotated ~240°. The release of Cy3-ADP accompanied a further step toward

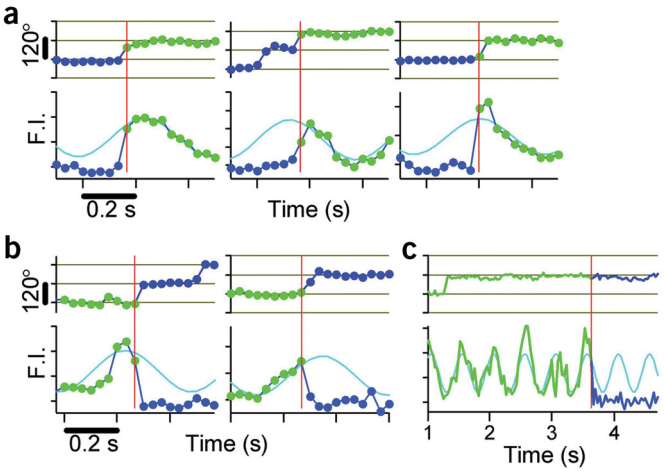

Figure 3 Timing between a rotational step of the γ subunit (upper panels) and binding or release of Cy3-nucleotide (lower panels). Examples of cases in which either binding or release occurred in a bright phase of the oscillation of fluorescence intensity (F.I.). (**a**) Binding. (**b**) Release. Dots correspond to video frames. (**c**) An exceptional case in which Cy3 disappeared without a step, probably as a result of photobleaching (see text). Red vertical lines show the video frame in which we judge binding or release of Cy3-nucleotide occurred.

360°, well within 0.5 s in 129 of the 142 cases, and confirmed to be within ±1 video frame when the release occurred in a bright phase of fluorescence (20 cases including **Fig. 3b**). The exceptional 13 cases (**Fig. 3c**) are probably due to photobleaching, because the 'releases' (disappearance of Cy3 fluorescence) without a step occurred mostly after an exceptionally long dwell time (at 200–240°, the angles at which even the GT mutant seemed prone to inhibition when Cy3-ADP was bound): the average dwell time in the exceptional cases was 16.9 s, whereas the dwell times before a release accompanying a step averaged 2.9 s. With the level of excitation intensity used in this study, the mean lifetime of photobleaching of Cy3-ATP was 8 s (T.N., data not shown), and thus long dwells are necessarily affected by photobleaching at some point. Apparently, therefore, release of ADP is also coupled to mechanical stepping. Binding and release of a nucleotide seem always to be tightly coupled to a mechanical event (120° rotation).

Kinetics of rotation driven by Cy3-ATP

The kinetics of the rotation driven by pure Cy3-ATP is basically similar to that driven by unlabeled ATP except that certain kinetic steps are slower. Cy3-ATP alone supported rotation for hundreds of revolutions, at least at such high concentrations as 20 μM. The average rate of rotation, however, was much lower with Cy3-ATP than with ATP (**Fig. 4a**,**b**). This difference is mainly due to the lower rate of Cy3-ATP binding: the average rotation rate was proportional to the nucleotide concentration for both Cy3-ATP and ATP, indicating that binding was rate-limiting in the concentration ranges examined; the binding rate k_{on} for Cy3-ATP was ~20-fold lower than k_{on} for ATP (**Fig. 4c**). The k_{on} for Cy3-ATP coincided with the hydrolysis rate in solution, corroborating the scheme of one Cy3-ATP molecule per 120°, as in the case of rotation of wild type F_1 by unlabeled ATP[7]. The k_{on} for unlabeled ATP in the GT mutant is small compared with that of the wild type, and was approximately half the bulk hydrolysis rate of this mutant in solution. In a modification of the method used in earlier studies, we used different buffer for the rotation assay (see Methods). This difference led to the lower rate of rotation by unlabeled ATP. Incidentally, an isomer of Cy3-ATP, 3′-*O*-Cy3-ATP, which normally coexists with the 2′ isomer that we used[13], gave a poor rotation rate (**Fig. 4c**), and the rotation often exhibited a long pause. We therefore purified the 2′ isomer from a mixture before use.

Because the rate is limited by substrate binding, rotation is expected to be stepwise, and so it was for Cy3-ATP as well: 120° steps were clearly resolved, as with unlabeled ATP (**Fig. 4b**). Remarkably, most of the 120° steps with Cy3-ATP were further resolved into substeps (**Fig. 4a**). Rotation traces showed six dwelling positions, from which the amplitudes of the substeps were obtained as 79 ± 7° (mean ± s.d.; n = 238 displacements in 19 F_1 molecules) and 41 ± 7° (n = 248). The distribution of substep sizes is given in **Supplementary Figure 3a** online. The appearance of video-rate substeps is not due to interaction of the Cy3 moiety with F_1, because EDA-ATP lacking the dye portion also showed the substep behavior (T.N., data not shown). In the rotation of wild-type F_1 driven by unlabeled ATP, substep amplitudes have been estimated as 90 ± 10° and 30 ± 10°, and the two substeps are contiguous within ~2 ms (ref. 12), beyond the temporal resolution of the ordinary video camera used in this study. Despite the difference in timing (and the small difference in amplitudes, which is within experimental uncertainty), we consider the substeps of ~80° and ~40° observed here to be of the same origin as the ~90° and ~30° substeps, for the following reason.

The dwells before an 80° substep, 0° dwells, were, on average, inversely proportional to the Cy3-ATP concentration, whereas the dwells after an 80° substep, 80° dwells, were independent of this concentration (**Fig. 4d**, and see **Supplementary Fig. 3b** online). These characteristics are common to the 0° dwells and 90° dwells in the ATP-driven rotation in the wild type[12], suggesting common underlying processes. The concentration dependence suggests that the 80° substep is triggered by binding of Cy3-ATP (to the site dictated by the γ subunit), and the 40° substep by a process subsequent to the binding, such as splitting of ATP in, or release of phosphate or ADP from, one of the three sites.

In experiments with the mixture of ATP and Cy3-ATP, the video-rate substeps are a signature of the site that carries Cy3-ATP. Below, we attempt an analysis using this signature, assuming that the same chemomechanical sequence occurs in F_1-ATPase whether it is driven by ATP or Cy3-ATP. We refer to previous 90° and 30° substeps as 80° and 40° substeps.

40° substep governed by site –1

Here we analyze the sequence of events induced by (infrequent) binding of Cy3-ATP during rotation in a mixture of Cy3-ATP and excess unlabeled ATP. The first event after binding was 120° stepping of the γ subunit, as already stated. Let the first step be from 0° to 120°: we designate the angle of the γ subunit (the bead duplex) immediately before binding of Cy3-ATP as 0° (**Fig. 2b**, middle panel). While the Cy3-ATP was still bound, the motor made another step toward ~240°. A closer look revealed that the second steps were often resolved into 80° and 40° substeps (**Fig. 2c**,**d**), reminiscent of the substeps seen in the rotation by pure Cy3-ATP. The 40° substep from 200° to 240° was not always clear because of noise, but a tendency to linger around 200° was noticeable in most cases (**Fig. 2b**; see **Supplementary Fig. 4** online for averages of the step record).

Our interpretation here is that all 120° steps are composed of 80° and 40° substeps, as in the wild type F_1 driven by unlabeled ATP[12], and that only substeps from 200° to 240° are discerned at the video rate because they are delayed by slow reaction(s) in the site hosting the Cy3-ATP or Cy3-nucleotide. If we call the catalytic site that has most recently bound ATP site 0, the site that governs the substep behavior is site –1, the site that bound ATP one step earlier.

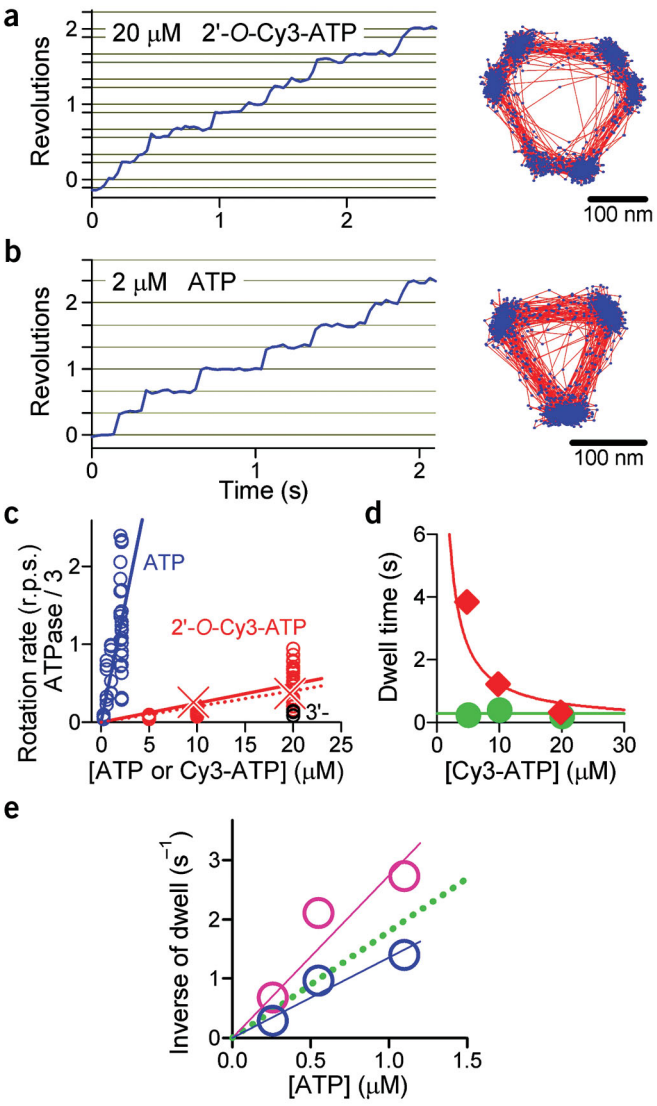

Figure 4 F_1 rotation driven by Cy3-ATP. (**a**) Left, a time course of F_1 rotation in 100% 2′-*O*-Cy3-ATP. Horizontal gray lines are 80° and 40° apart. Right, the trace of bead rotation for 70 s. Centroid positions at all video frames (blue dots) are connected by red lines. (**b**) A rotation time course of F_1 (left) and corresponding trace for 70 s (right) in 100% unlabeled ATP. (**c**) Time-averaged rotation rates by ATP (blue circles), 2′-*O*-Cy3-ATP (red) and 3′-*O*-Cy3-ATP (black). Samples that showed clear 120° steps (or 80° and 40° substeps) during 5–20 consecutive revolutions were chosen. Solid lines show fits with k_{on} (3× rotational rate) of 1.8×10^6 $M^{-1}s^{-1}$ (blue) and 0.073×10^6 M^{-1} s^{-1} (red), assuming consumption of three nucleotides per revolution. The rate of 2′-*O*-Cy3-ATP hydrolysis in solution (red crosses and red dashed line), 0.06×10^6 M^{-1} s^{-1}, coincided with rotation rate. (**d**) ATP dependence of average dwell times before an 80° substep ('0° dwell' $\tau_{0°}$, red diamonds) and dwell times after an 80° substep ('80° dwell' $\tau_{80°}$, green circles). Red line shows fit with $\tau_{0°} = (0.08 \times 10^6\ M^{-1}\ s^{-1})^{-1} \times [\text{Cy3-ATP}]^{-1}$, which agrees with the estimation in **c**, and green line, $\tau_{80°}$ = constant = 0.3 s. (**e**) ATP dependence of the average dwell time in the mixture. Pink circles are at 120° (see **Fig. 2b** and text for angle definition) (total n at three different ATP concentrations = 138) and blue circles, 200–240° (n = 122). Green line is the binding rate of unlabeled ATP estimated from rotation in 100% ATP (see **c**).

Both the 80° substep from 120° to 200° and the next 80° substep from 240° to 320° (part of the observed 120° step from 240° to 360°) must be driven by ATP binding, if the presence of Cy3 fluorophore in bound nucleotide does not alter the basic reaction sequence. In support of this, the rates of occurrence of these substeps, estimated as the inverse of dwell times at 120° and at 200–240° (the interval between a 120–200° substep and the next 240–360° step), were each proportional to the concentration of unlabeled ATP, and both approximately agreed with the rate of ATP binding (**Fig. 4e**), allowing for relatively large uncertainties due to low counting statistics (the ATP-independent dwell time at 200° is partially responsible for the apparently longer dwell time at 200–240°).

DISCUSSION

In the scheme that emerges (**Fig. 5a**,**b**) at least two of the three catalytic sites are always filled with a nucleotide, and thus the occupancy must be two when F_1 is waiting for the next ATP molecule. Four successive ATP-waiting states are shown (**Fig. 5a**), with the step from 0° to 120° driven by binding of Cy3-ATP. Events between 120° and 240° are detailed (**Fig. 5b**): (I) ATP binds to the remaining empty site of the β subunit. We call this site, as before, site 0. (II) The binding drives the 80° substep from 120° to 200°. (III) Before the γ subunit makes the next substep from 200° to 240°, reaction(s) must take place at site –1. This rate-limiting reaction must take place at site –1, based on the Cy3-ATP's slow substep signature. Candidates of the rate-limiting reactions include hydrolysis at, or release of phosphate from, site –1, but not the release of ADP from this site (because Cy3 remained bound at least until 240°). (IV) A 40° substep occurs, and the γ subunit reaches 240°. There, the F_1 motor waits for the next ATP molecule to initiate the same sequence (except that event III is now fast).

At some point between events I and IV, ADP must be released from site –2 to vacate that site for the next ATP. Unfortunately, we have not been able to determine the timing of ADP release because substeps were not resolved in the step synchronous with the release of Cy3-ADP. ADP release is unlikely to be after event IV, because in the wild-type F_1 rotating at a high concentration of unlabeled ATP, a 40° substep is followed by the next 80° substep within 0.1 ms: as soon as the 40° substep is complete, the motor is ready to bind the next ATP, and thus one site must be empty[12]. A probable timing for ADP release is during the 40° substep (IV), because F_1 inhibited by failing to release MgADP has been shown to pause around ~80° (ref. 22). Also, because ATP binding produces the major substep of 80°, or the major conformational change of F_1, we do not expect complete mechanical silence for the essentially reverse process of ADP release: some rotation accompanying ADP release is quite probable. A possible scenario could consist of (i) hydrolysis in, or the release of phosphate from, site –1 initiating a 40° substep; (ii) site –2 sensing the slight movement of the γ subunit and (iii) releasing ADP, which drives (iv) the rest of the 40° substep. Another possible timing for ADP release is during the 80° substep (II) ATP binding to site 0 initiates this substep, and ADP release from site –2 helps complete the 80° substep. In this scenario, site occupancy is always two except for the brief (<0.1 ms) interchanging period.

Other, more complex scenarios cannot be dismissed, because a small-amplitude rotation, for example by 10°, would not have been detected in our analyses. In this regard, the difference between the 80° substep observed here and the previous 90° substep[12] might be important. For example, ATP binding to site 0 induces a 80° substep, ATP hydrolysis in site –1 induces another 10° substep, and phosphate release[26] from site –1 and/or ADP release from site –2 drives the last 30° rotation. Consistent with this, a slowly hydrolyzed substrate ATP-γ-S produces 80° substeps at video rate[27]. A notable feature is the

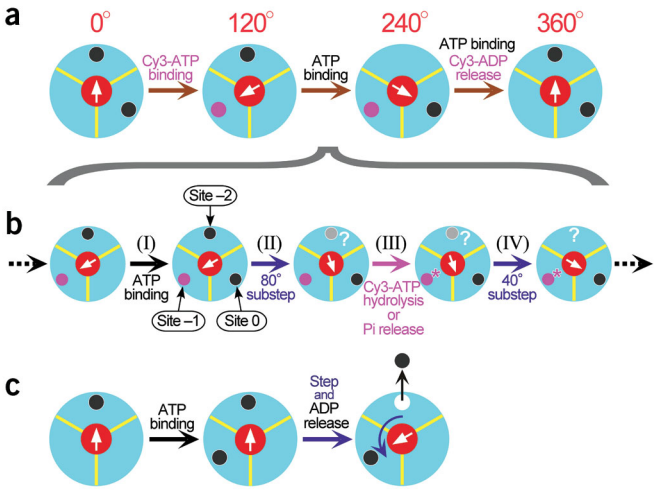

Figure 5 Mechanism of F_1 rotation. (**a**) Rotation scheme consistent with **Figure 2**. Four successive ATP-waiting states are shown. (**b**) Events between 120° and 240°. Nucleotide occupancy in schemes **a** and **b** alternates between two and three. (**c**) An alternative scheme in which the occupancy alternates between one and two (see Discussion).

coupling of rotation with ATP hydrolysis, which will help achieve a high efficiency in the reverse reaction of ATP synthesis[10].

According to the scheme shown here (**Fig. 5b**), at least two catalytic sites (two β subunits) carry out major functions in rotating the γ subunit by 120°. One is the site that has just bound ATP (site 0), which produces the 80° substep. The other is site –1, which controls the timing of (and possibly drives) the 40° substep. As stated above, site –2 also probably assists rotation by releasing ADP. Coordination among the three sites has been proposed[2,3], and now this coordination is beginning to be unraveled.

A current debate regarding F_1 rotation concerns whether the motor operates under bi- or tri-site mode[10,28,29]. In the simplest definition, bi-site is the mode in which the nucleotide occupancy of the three catalytic sites alternates between one and two (**Fig. 5c**), whereas the tri-site mode involves alternation between two and three (**Fig. 5a**,**b**). The bi-site view has recently been challenged[11,28] with the claim that, on the basis of site occupancy estimated from fluorescence quenching of tryptophan residues introduced in the catalytic sites, hydrolysis and rotation do not occur until a third site binds ATP, and thus bi-site activity does not exist. The present study also supports a tri-site scheme, because Cy3-nucleotide remained bound at least for 240° of rotation of the γ subunit, or until two more ATP molecules bound and a step from 240° to 360° (320°) occurred. Cy3-ATP always bound to the correct β subunit, consistent with a tri-site scheme that leaves only one vacant site for binding, although the asymmetric β could also dictate a particular site to bind ATP in the bi-site mode. We cannot completely exclude the possibility that Cy3-ADP may be stickier than ADP and have a greater tendency to linger in the catalytic site; thus only Cy3-nucleotide, and not nucleotide, might remain bound for 240° or more.

The major questions remaining are when, and from which site, phosphate is released, and what is the timing of ADP release. To answer these questions, techniques must be developed to allow high-speed imaging of fluorescent ATP, as well as detection and resolution of two or more fluorescent ATP molecules on one F_1 molecule. We emphasize that orientation imaging, used here to distinguish among three catalytic sites, is a powerful tool for studying multisite enzymes in general, and also for detecting local conformational changes in different parts of a protein and/or RNA machine (through fluorophore angle changes) simultaneously with an assessment of its function (through a large tag such as a bead or a bead duplex).

METHODS

Proteins. The GT mutant of the $\alpha_3\beta_3\gamma$ subcomplex was derived from a thermophilic *Bacillus* strain PS3 F_1-ATPase and contained the following mutations: β-G181A (ref. 30) and β-T165S (ref. 20) for minimizing MgADP inhibition; α-C193S, γ-S107C and γ-I210C for specific biotinylation of the γ subunit[8,12]; β-His_{10} at the N terminus[5], α-W463F and β-Y341W (refs. 31–33). The GT mutant showed a V_{max} of 250 ± 20 (mean ± s.d.) $s^{-1}$and a K_m of 37 ± 10 μM for the hydrolysis reaction at 25 °C in buffer A (50 mM KCl, 2 mM $MgCl_2$, 10 mM MOPS-KOH, pH 7.0; the GT mutant does not require lauryldodecylamine oxide (LDAO) for hydrolysis measurement because of its resistance to MgADP inhibition), which are comparable to the values of 247 s^{-1} and 19 μM for the wild type F_1 in the presence of LDAO in buffer A[12]. In buffer B (2 mM $MgCl_2$, 20 mM potassium phosphate, pH 8.0) used for the rotation assay, V_{max} was 210 ± 10 $s^{-1}$and K_m 50 ± 3 μM, yielding an apparent k_{on} for ATP binding of V_{max} / K_m = 4.2×10^6 $M^{-1}s^{-1}$, which is smaller than k_{on} of 13×10^6 $M^{-1}s^{-1}$ for wild type F_1 in buffer A with LDAO[12]. k_{on} from the rotation assay (**Fig. 4c**) is half these values, presumably because of surface hindrance.

Rotation assay. 1.4% (w/v) amino-modified polystyrene beads (amino-modified, 0.22 μm in diameter; Polysciences) were modified with 1 mg ml^{-1} biotin-$(AC_5)_2$-Sulfo-Osu (Dojindo) at room temperature for 4 h, and unreacted biotin was removed by centrifugation (20,000*g* for ~10 min). Then, 0.2 mg ml^{-1} streptavidin (Sigma) was added, and excess streptavidin was washed away. Biotin (biotin-$PEAC_5$-maleimide; Dojindo) was coupled to cysteines in the γ subunit of F_1 by a 30-min incubation at room temperature at 1–8 μM F_1 at F_1/biotin = 1:2. To observe rotation, ~100 pM F_1 in buffer A was infused into a flow chamber comprising two glass coverslips; the top coverslip was coated with 3-glycidyloxypropyl-trimethoxysilane (Fluka) to avoid binding of the protein, and the bottom one had been cleaned in 10 M KOH overnight and washed with distilled water. F_1 attached nonspecifically to the bottom surface. After 2 min, the chamber was washed with 20 mM potassium phosphate, and then the streptavidin-coated beads at 0.1% (w/v) were infused. Avidin on the beads specifically attached to the γ subunit in a single F_1, whereas $\alpha_3\beta_3$ subcomplexes were immobilized on the surface; therefore, stepping between $\alpha_3\beta_3$ and γ was visualized as displacement of beads. For simultaneous observation of Cy3-ATP binding, buffer B plus the oxygen scavenger system[34], 0.5% (v/v) 2-mercaptoethanol, 35–65 nM Cy3-ATP, the desired amount of unlabeled ATP, 0.02 mg ml^{-1} creatine kinase, 0.08 mg ml^{-1} creatine phosphate, was infused. For rotation in Cy3-ATP, buffer B only with the desired amount of Cy3-ATP was infused instead. In both cases, rotating beads often showed large-angle fluctuations, and these did not show clean steps. For analysis, we selected those that showed steady and consistent 120° steps (**Figs. 2** and **4a**,**b**). A possible reason for the slightly slower rotation of this GT mutant by authentic ATP as compared with the wild type is that the selected F_1 molecules were probably attached to the surface firmly and thus may have been impeded by surface interactions. Observations were made at 23 ± 2 °C.

Cy3-ATP and its hydrolysis by F_1. Cy3-ATP and its isomers were synthesized and purified as reported[13]. The bulk hydrolysis rate of 2′-*O*-Cy3-ATP was measured by mixing 10 nM F_1 with 2′-*O*-Cy3-ATP in buffer B. Aliquots of the reaction solution were then taken and quenched with buffer C (20% (v/v) acetonitrile and 0.6 M $NH_4H_2PO_4$, pH 4.2–4.3). They were analyzed by anion-exchange chromatography (Partisil 10 SAX; Whatman) in buffer C and quantified by the integrated fluorescence intensity of Cy3-ADP. The hydrolysis rate was determined from the amount of 2′-*O*-Cy3-ADP present after the first 1 min of reaction, which was <3% of the initial Cy3-ATP.

Microscopy and analyses. For imaging Cy3-ATP, a green laser beam (wavelength 532 nm; Compass, Coherent) was introduced into an Olympus IX-70 microscope. The beam power at the base of the objective (60×; numerical aperture 1.45; Olympus) was 0.16–0.20 mW for 100 μm^2 illumination at the sample plane. Polarization of the evanescent wave in the image plane was

rotated at a constant speed (0.9990 r.p.s.). For quantitative analysis of the intensity of Cy3, the average intensity over a 0.78-μm square enclosing the center of Cy3 was calculated[8]. The background intensity either before Cy3-ATP binding or after Cy3-ADP release was averaged for 10–30 cycles, and the averaged intensity was subtracted from the Cy3 signal. To determine the Cy3 angle, the intensity record corresponding to a binding event (judged visually) was fitted with a 1.9980-Hz cosine curve with three variables: the amplitude, offset and phase. The difference between this phase and that of the excitation polarization gave the Cy3 angle. For bead imaging, a halogen lamp illuminated the condenser through a 660- to 880-nm filter. The fluorescence (Cy3-ATP) and bright-field (bead duplex) images were separated with a dichroic mirror and recorded with two electronically synchronized cameras[34,35]. The diagram of the microscope system is given (**Supplementary Fig. 1** online). Typically, one record continued for 0.5–1 h, during which 3–20 Cy3-ATP molecules bound to an F_1 molecule. For each F_1 molecule, the angle between the catalytic sites and bead orientations is different because the bead duplex can attach to the γ subunit at any angle. Therefore, in the illustration (**Fig. 2e**), a constant angle values apecific for each molecule have been subtracted from the abscissa and ordinate, such that the bead angles close to the 3 o'clock position average 0°, and the corresponding Cy3 angles also average 0°. Cy3 angles have been chosen from the 180° redundancies such that they match the bead angles. For Cy3-ATP binding (**Fig. 3a**), the 8 exceptions of the 163 cases were as follows: 5 cases in which the bead duplex did not rotate during the whole binding event, 1 case in which Cy3-ATP bound in the middle of the dwell time between two steps (we dismissed these events as binding to a nearby F_1 molecule or as nonspecific binding to the glass surface) and 2 cases in which binding of Cy3-ATP induced a backward 120° step[7].

Note: Supplementary information is available on the Nature Structural & Molecular Biology website.

ACKNOWLEDGMENTS

We thank R. Yasuda, K. Adachi and H. Itoh for technical assistance and critical discussion; R. Nakamori and Y. Funamoto for technical assistance; D.R. Trentham for initiation of our collaboration; T. Masaike, B. Brenner and H. Kojima for critical discussion; M. Shio, K. Abe and I. Sase for the microscope techniques; and M. Uno and H. Umezawa for management of laboratories and collaboration. This work was supported in part by grants-in-aid from the Ministry of Education, Culture, Sports, Science and Technology of Japan, and by a Core Research for Evolutional Science and Technology (CREST) grant.

COMPETING INTERESTS STATEMENT

The authors declare that they have no competing financial interests.

Received 27 August; accepted 13 November 2003
Published online at http://www.nature.com/natstructmolbiol/

1. Abrahams, J.P., Leslie, A.G., Lutter, R. & Walker, J.E. Structure at 2.8 Å resolution of F_1-ATPase from bovine heart mitochondria. *Nature* **370**, 621–628 (1994).
2. Boyer, P.D. The binding change mechanism for ATP synthase—some probabilities and possibilities. *Biochim. Biophys. Acta* **1140**, 215–250 (1993).
3. Boyer, P.D. The ATP synthase—a splendid molecular machine. *Annu. Rev. Biochem.* **66**, 717–749 (1997).
4. Yoshida, M., Muneyuki, E. & Hisabori, T. ATP synthase—a marvelous rotary engine of the cell. *Nat. Rev. Mol. Cell Biol.* **2**, 669–677 (2001).
5. Noji, H., Yasuda, R., Yoshida, M. & Kinosita, K. Jr. Direct observation of the rotation of F_1-ATPase. *Nature* **386**, 299–302 (1997).
6. Noji, H. *et al.* Purine but not pyrimidine nucleotides support rotation of F_1-ATPase. *J. Biol. Chem.* **276**, 25480–25486 (2001).
7. Yasuda, R., Noji, H., Kinosita, K. Jr. & Yoshida, M. F_1-ATPase is a highly efficient molecular motor that rotates with discrete 120° steps. *Cell* **93**, 1117–1124 (1998).
8. Adachi, K. *et al.* Stepping rotation of F_1-ATPase visualized through angle-resolved single-fluorophore imaging. *Proc. Natl. Acad. Sci. USA* **97**, 7243–7247 (2000).
9. Boyer, P.D. Catalytic site forms and controls in ATP synthase catalysis. *Biochim. Biophys. Acta* **1458**, 252–262 (2000).
10. Kinosita, K. Jr., Yasuda, R., Noji, H. & Adachi, K. A rotary molecular motor that can work at near 100% efficiency. *Phil. Trans. R. Soc. Lond. B* **355**, 473–489 (2000).
11. Weber, J. & Senior, A.E. ATP synthase: what we know about ATP hydrolysis and what we do not know about ATP synthesis. *Biochim. Biophys. Acta* **1458**, 300–309 (2000).
12. Yasuda, R., Noji, H., Yoshida, M., Kinosita, K. Jr. & Itoh, H. Resolution of distinct rotational substeps by submillisecond kinetic analysis of F_1-ATPase. *Nature* **410**, 898–904 (2001).
13. Oiwa, K. *et al.* Comparative single-molecule and ensemble myosin enzymology: sulfoindocyanine ATP and ADP derivatives. *Biophys. J.* **78**, 3048–3071 (2000).
14. Tokunaga, M., Kitamura, K., Saito, K., Iwane, A.H. & Yanagida, T. Single molecule imaging of fluorophores and enzymatic reactions achieved by objective-type total internal reflection fluorescence microscopy. *Biochem. Biophys. Res. Commun.* **235**, 47–53 (1997).
15. Funatsu, T., Harada, Y., Tokunaga, M., Saito, K. & Yanagida, T. Imaging of single fluorescent molecules and individual ATP turnovers by single myosin molecules in aqueous solution. *Nature* **374**, 555–559 (1995).
16. Ishijima, A. *et al.* Simultaneous observation of individual ATPase and mechanical events by a single myosin molecule during interaction with actin. *Cell* **92**, 161–171 (1998).
17. Ha, T., Enderle, T., Chemla, S., Selvin, R. & Weiss, S. Single molecule dynamics studied by polarization modulation. *Phys. Rev. Lett.* **77**, 3979–3982 (1996).
18. Sase, I., Miyata, H., Ishiwata, S. & Kinosita, K. Jr. Axial rotation of sliding actin filaments revealed by single-fluorophore imaging. *Proc. Natl. Acad. Sci. USA* **94**, 5646–5650 (1997).
19. Axelrod, D. Total internal reflection fluorescence at biological surfaces. in *Noninvasive Techniques in Cell Biology* (eds. Foskett, J.K. & Grinstein, S.) 93–127 (Wiley-Liss, New York, 1990).
20. Jault, J.M. *et al.* The $\alpha_3\beta_3\gamma$ subcomplex of the F_1-ATPase from the thermophilic bacillus PS3 with the βT165S substitution does not entrap inhibitory MgADP in a catalytic site during turnover. *J. Biol. Chem.* **271**, 28818–28824 (1996).
21. Matsui, T. *et al.* Catalytic activity of the $\alpha_3\beta_3\gamma$ complex of F_1-ATPase without noncatalytic nucleotide binding site. *J. Biol. Chem.* **272**, 8215–8221 (1997).
22. Hirono-Hara, Y. *et al.* Pause and rotation of F_1-ATPase during catalysis. *Proc. Natl. Acad. Sci. USA* **98**, 13649–13654 (2001).
23. Vale, R.D. & Oosawa, F. Protein motors and Maxwell's demons: does mechanochemical transduction involve a thermal ratchet? *Adv. Biophys.* **26**, 97–134 (1990).
24. Astumian, R.D. & Bier, M. Fluctuation driven ratchets: molecular motors. *Phys. Rev. Lett.* **72**, 1766–1769 (1994).
25. Hunt, A.J., Gittes, F. & Howard, J. The force exerted by a single kinesin molecule against a viscous load. *Biophys. J.* **67**, 766–781 (1994).
26. Masaike, T., Muneyuki, E., Noji, H., Kinosita, K. Jr. & Yoshida, M. F_1-ATPase changes its conformations upon phosphate release. *J. Biol. Chem.* **277**, 21643–21649 (2002).
27. Shimabukuro, K. *et al.* Catalysis and rotation of F_1 motor: cleavage of ATP at the catalytic site occurs in 1 ms before 40° substep rotation. *Proc. Natl. Acad. Sci. USA* **100**, 14731–14736 (2003).
28. Weber, J. & Senior, A.E. Bi-site catalysis in F_1-ATPase: does it exist? *J. Biol. Chem.* **276**, 35422–35428 (2001).
29. Boyer, P.D. Catalytic site occupancy during ATP synthase catalysis. *FEBS Lett.* **512**, 29–32 (2002).
30. Masaike, T. *et al.* Rotation of F_1-ATPase and the hinge residues of the β subunit. *J. Exp. Biol.* **203**, 1–8 (2000).
31. Dou, C., Fortes, P.A. & Allison, W.S. The $\alpha_3(\beta Y341W)_3\gamma$ subcomplex of the F_1-ATPase from the thermophilic *Bacillus* PS3 fails to dissociate ADP when MgATP is hydrolyzed at a single catalytic site and attains maximal velocity when three catalytic sites are saturated with MgATP. *Biochemistry* **37**, 16757–16764 (1998).
32. Ren, H. & Allison, W.S. Substitution of $betaGlu_{201}$ in the $\alpha_3\beta_3\gamma$ subcomplex of the F_1-ATPase from the thermophilic *Bacillus* PS3 increases the affinity of catalytic sites for nucleotides. *J. Biol. Chem.* **275**, 10057–10063 (2000).
33. Mitome, N. *et al.* The presence of phosphate at a catalytic site suppresses the formation of the MgADP-inhibited form of F_1-ATPase. *Eur. J. Biochem.* **269**, 53–60 (2002).
34. Nishizaka, T., Seo, R., Tadakuma, H., Kinosita, K. Jr. & Ishiwata, S. Characterization of single actomyosin rigor bonds: load dependence of lifetime and mechanical properties. *Biophys. J.* **79**, 962–974 (2000).
35. Nishizaka, T., Miyata, H., Yoshikawa, H., Ishiwata, S. & Kinosita, K. Jr. Unbinding force of a single motor molecule of muscle measured using optical tweezers. *Nature* **377**, 251–254 (1995).